Наносистеми, наноматеріали, нанотехнології
Nanosistemi, Nanomateriali, Nanotehnologii
2023, т. 21, № 3, сс. 617–630

PACS numbers: 78.20.Ci, 78.40.Me, 78.67.Sc, 82.35.Lr, 82.35.Np, 87.19.xb, 87.85.Rs

Synthesis and Improved Optical Characteristics of Biopolymer Blend Doped with Iron-Oxide Nanoparticles for Optics and Biomedical Applications

Majeed Ali Habeeb[1], Ahmed Hashim[1], and Ranya Mahmood Mohammed[2]

[1]*College of Education for Pure Sciences,*
Department of Physics,
University of Babylon,
Hillah, Iraq
[2]*Al Zahraa University for Women,*
Karbala-Baghdad Str.,
Holy City of Karbala, Iraq

The current study is focused on the enhancement of the optical characteristics of polyethylene-oxide and polyvinyl-alcohol blend with different weight percentages of iron-oxide nanoparticles (0, 1.5%, 3%, 4.5%, and 6% wt.) created by casting technique. Optical examinations show that the absorbance of PEO/PVA/Fe_2O_3 nanocomposites increases with increase of iron-oxide nanoparticles' content, while the energy gap of PEO/PVA/Fe_2O_3 nanocomposites is dropped from 3.79 eV to 3.38 eV and from 2.79 eV to 2.18 eV for allowed and forbidden indirect transitions, respectively, when the addition of iron-oxide nanoparticles reaches 6 wt.%. This feature can play a vital role in enabling PEO/PVA/Fe_2O_3 nanocomposites for future optoelectronics applications. The refractive index, extinction coefficient, dielectric constant and optical conductivity increase with increasing the concentration of iron-oxide nanoparticles. The antibacterial properties of the PEO/PVA/Fe_2O_3 nanocomposites are investigated against *E. coli* bacteria. Experimental results show that the inhibition zone diameter increases with increase of iron-oxide nanoparticles' concentration. Finally, PEO/PVA/Fe_2O_3 nanocomposites have a good antibacterial activity.

Поточне дослідження зосереджено на поліпшенні оптичних характеристик суміші поліоксиетилену (ПОЕ) та полівінілового спирту (ПВС) з різним ваговим відсотком наночастинок оксиду Феруму (0, 1,5%, 3%, 4,5% і 6% мас.), створених методом лиття. Оптичні дослідження показують, що поглинання нанокомпозитів ПОЕ/ПВС/Fe_2O_3 зростає зі збільшенням вмісту наночастинок оксиду Феруму, тоді як енергетична щілина нанокомпозитів ПОЕ/ПВС/Fe_2O_3 зменшується з 3,79 еВ до 3,38

еВ та з 2,79 еВ до 2,18 еВ для дозволеного та забороненого непрямих переходів відповідно, коли додавання наночастинок оксиду Феруму досягає 6 мас.%. Ця особливість може відігравати життєво важливу роль у створенні нанокомпозитів ПОЕ/ПВС/Fe_2O_3 для майбутніх застосувань в оптоелектроніці. Показник заломлення, коефіцієнт екстинкції, діелектрична проникність і оптична провідність збільшуються зі збільшенням концентрації наночастинок оксиду Феруму. Досліджено антибактеріальні властивості нанокомпозитів ПОЕ/ПВС/Fe_2O_3 щодо бактерій *E. coli*. Експериментальні результати показують, що діяметер зони інгібування збільшується зі збільшенням концентрації наночастинок оксиду Феруму. Нарешті, нанокомпозити ПОЕ/ПВС/Fe_2O_3 мають гарну антибактеріяльну активність.

Key words: bionanocomposites, iron-oxide nanoparticles, optical properties, antibacterial activity.

Ключові слова: біонанокомпозити, наночастинки оксиду Феруму, оптичні властивості, антибактеріяльна активність.

(Received 10 February, 2023)

1. INTRODUCTION

Nanocomposites (NCs) consist of two or more materials where one of these materials has nanoscale. The addition of inorganic nanoparticles (NPs) into a polymer matrix will change both properties from inorganic nanoparticles and polymer to be enhanced and hence advanced new functions can be generated to the nanocomposites [1, 2]. The nanocomposites' applications are quite promising in the fields of microelectronic packaging, medicine, automobiles, optical integrated circuits, drug delivery, injection moulded products, sensors, membranes, aerospace, packaging materials, coatings, fire retardants, adhesives, consumer goods, *etc.* [3].

Poly(ethylene oxide) (PEO) is most often regarded as a major problem in real working systems, since the ionic conduction has been shown to take place mainly in the amorphous phase. The suppression of crystallinity of polymer chains improves the polymer chain mobility, which, in turn, leads to better ionic conduction. Polymer blending is one of the effective methods to reduce the crystalline content and enhance the amorphous content. Polymer blends often exhibit properties, which are superior to the individual component polymers [4, 5].

Poly(ethylene oxide) has attracted attention in recent years due to their solubility in water, biodegradability, non-toxicity, and biocompatibility. It has numerous applications, such as agricultural films, paper coating, textile fibres, and electronic devices [6].

Poly(vinyl alcohol) (PVA) is a biodegradable synthetic polymer, which is a kind of thin film material with excellent performance and wide application. In addition, the research results on the composite film of polyvinyl alcohol (PVA) with a variety of materials, including essential oils, modified nanomaterials, *etc.*, proved its good packaging performance, and the existence of film pores and the size of the loading affect the number of antimicrobial agents, thus affecting the antibacterial properties of the film [7, 8].

Polyvinyl alcohol offers a combination of excellent film forming and binder characteristics, along with insolubility in cold water and organic solvents. This combination of characteristics is useful in a variety of applications. Moreover, it contains a carbon backbone with hydroxyl groups attached to methane carbons. These hydroxyl groups can be a source of hydrogen bonding, hence the assistance in the formation of polymer blends. PVA is harmless and has excellent thermal stability, creation it a hopeful candidate to be used in biotechnology and biomedicine fields [9, 10].

The iron oxide (Fe_2O_3), the most common oxide of iron, has the important magnetic properties too. From the viewpoint of the basic research, iron(III) oxide is a convenient compound for the general study of polymorphism and the magnetic and structural phase transitions of nanoparticles. The existence of amorphous Fe_2O_3 and four polymorphs (alpha, beta, gamma and epsilon) is well-established [11]. The most frequent polymorphs structure 'alpha' (hematite) having a rhombohedral–hexagonal, prototype corundum structures and cubic spinel structure 'gamma' (maghemite) have been found in nature. At a temperature of 650°C, hematite turns into Fe_3O_4 with a high energy loss [12]. Hematite has strongly antiferromagnetic properties. Gamma-Fe_2O_3 (maghemite) is the ferrimagnetic cubic form of Fe(III) oxide, and it differs from the inverse spinel structure of magnetite through vacancies on the cation sublattice. In time, at room temperature, the maghemite turns into hematite crystalline structure. Maghemite has the same crystalline structure like Fe_3O_4 (magnetite) [13].

This paper deals with synthesis and characteristics of PEO–PVA–Fe_2O_3 nanocomposites for use in optoelectronics and biomedical fields.

2. EXPERIMENTAL PART

Films of nanocomposites were made from polyvinyl alcohol–polyethylene oxide and iron-oxide nanoparticles using the casting method, which involved dissolving pure PEO and PVA (50/50) in 40 ml of distilled water for 40 minutes with a magnetic stirrer at temperature of 70°C to produce a more uniform solution. Iron-oxide

nanoparticles were added to the polymer blend at concentrations of 0%, 1.5%, 3%, 4.5%, and 6% wt. When the solution was dried during 4 days at room temperature, polymer nanocomposites were formed. The optical properties of PEO/PVA/Fe_2O_3 nanocomposites in the wavelength range 200–100 nm were measured by UV/1800/ Shimadzu spectrophotometer. The agar well diffusion method was used to test the antimicrobial activity of the nanocomposite films against *Escherichia coli* bacteria.

The absorbance is calculated from equation [14]

$$A = I_A/I_0, \tag{1}$$

where I_A represents the light intensity absorbed by the medium, and I_0 represents the incident light intensity.

The following equation is used to determine the transmittance (T) [15]:

$$A = \log(1/T), \tag{2}$$

Absorption coefficient (α) is calculated by the equation [16]

$$\alpha = 2.303(A/t), \tag{3}$$

where A is the absorbance, t is the thickness of sample.

For indirect transition model, following Ref. [17],

$$\alpha h\nu = B(h\nu - E_g)^x \tag{4}$$

can be computed; here, B is a constant, $h\nu$ is the photon energy, E_g is the optical energy band gap; $x = 3$ for the forbidden indirect transition and $x = 2$ for allowed indirect transition.

Refractive index (n) is determined by following equation [18]:

$$n = \sqrt{\frac{4R - k^2}{(R-1)^2}} - \frac{R+1}{R-1}, \tag{5}$$

where R is a reflection coefficient.

The extinction coefficient (k) is determined by the following equation [19]:

$$k = \alpha\lambda/(4\pi), \tag{6}$$

where λ is the wavelength of incident light.

The dielectric constant is classified in two parts: real (ε_1) and imaginary (ε_2) ones. It can be computed each of the real and imaginary parts of dielectric constant (ε_r and ε_{im}) by the following equations

[20, 21]:

$$\varepsilon_1 = n^2 - k^2, \tag{7}$$

$$\varepsilon_2 = 2nk. \tag{8}$$

The optical conductivity has been determined by [22]

$$\sigma \quad \alpha nc/(4\pi), \tag{9}$$

where c is light velocity.

3. RESULTS AND DISCUSSION

3.1. Absorbance and Transmittance

Figure 1 displays the variation of optical absorbance with wavelength for PEO/PVA/Fe_2O_3 nanocomposites. This figure notes that the spectra reveal that all these films show more absorbance in ultraviolet region. All nanocomposites show that low absorbance in the visible region. This behaviour can be explained as to interact with atoms, thus, the photon will be transmitted [23, 24]. If the wavelength decreases, the interaction between incident photon and material will occur, and the photon will be absorbed; the absorbance increases with increasing of weight percentages of the nanomaterials. This is due to absorption of the incident light by free electrons [25].

Figure 2 shows the transmittance of PEO/PVA/Fe_2O_3 nanocomposites with wavelength of photon. As shown in this figure, the

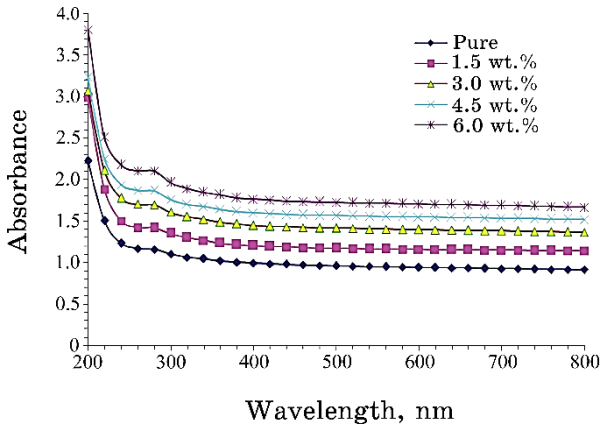

Fig. 1. Variation absorbance spectra of PEO/PVA/Fe_2O_3 nanocomposites with wavelength.

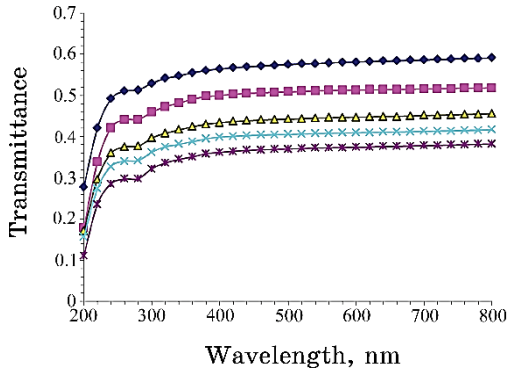

Fig. 2. Variation transmittance of PEO/PVA/Fe_2O_3 nanocomposites with wavelength.

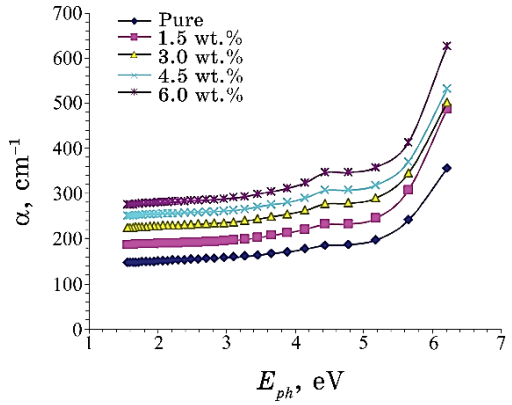

Fig. 3. Variation of absorption coefficient (α) of PEO/PVA/Fe_2O_3 nanocomposites with photon energy.

transmittance decreases with the increase in Fe_2O_3 nanoparticles; this is caused by the added Fe_2O_3 nanoparticles [26].

3.2. Absorption Coefficient (α) and Energy Gaps of the Allowed and Forbidden Transitions

The absorption coefficient (α) is calculated by using Eq. (3). Figure 3 shows that the absorption coefficient (α) as a function of the photon energy for the PVA/PEO blend with different concentration of Fe_2O_3 nanoparticles. It can be noted that absorption is low at low energy. This means that the possibility of electron transition is low because the energy of the incident photon is not sufficient to move the electron from the valence band to the conduction band ($h\nu < E_g$).

At high energies, absorption is greater; this shows that there is great possibility for electron transitions; consequently, the energy of incident photon is enough to move the electron from the valence band to the conduction band; this means that the energy of the incident photon is greater than the forbidden energy gap [27–29]. This one shows that the absorption coefficient assists in figuring out the nature of electron transition; when the values of the absorption coefficient is high $\alpha > 10^4$ cm^{-1} at high energies, it is expected that direct transition of electron occurs; the energy and moment are maintained by the electrons and photons, on the other hand, when the values of the absorption coefficient is low $\alpha < 10^4$ cm^{-1} [30].

The allowed and forbidden indirect transition energy gaps have been calculated by using Eq. (4). Figures 4 and 5 show the relation-

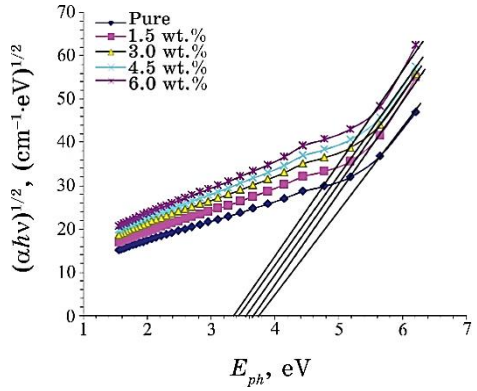

Fig. 4. Variation of $(\alpha h\nu)^{1/2}$ of PEO/PVA/Fe_2O_3 nanocomposites with photon energy.

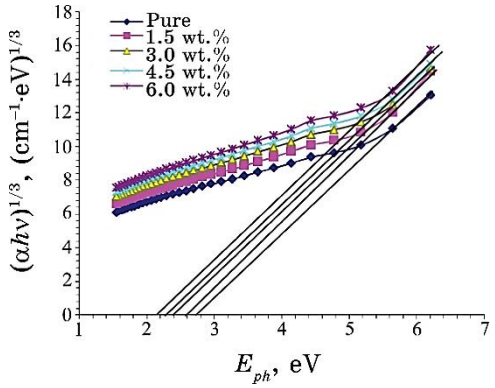

Fig. 5. Variation of $(\alpha h\nu)^{1/3}$ of PEO/PVA/Fe_2O_3 nanocomposites with photon energy.

ship between $(\alpha h\nu)^{1/2}$, $(\alpha h\nu)^{1/3}$ and the photon energy of PEO/PVA/Fe_2O_3 NCs. The values of the energy gap decrease as the percentage of Fe_2O_3 nanoparticles increases. The creation of localized levels inside the forbidden energy gap is responsible for this occurrence [31–33].

3.3. Extinction Coefficient and Refractive Index

Figure 6 shows the extinction coefficient (k) of PEO/PVA/Fe_2O_3 nanocomposites as a function of wavelength. It can be noted that k has low values at low values of concentration, but it increases with the increasing of the concentration of Fe_2O_3 nanoparticles. This is attributed to increased absorption coefficient with the increase of

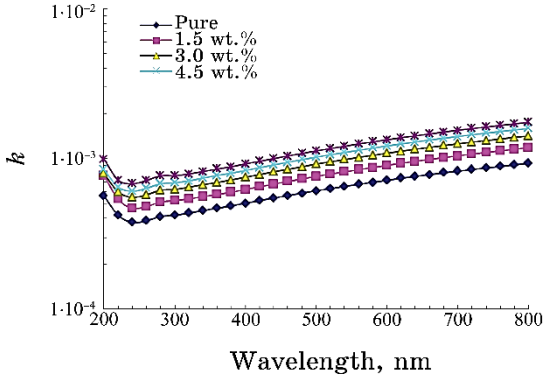

Fig. 6. Variation of extinction coefficient of PEO/PVA/Fe_2O_3 nanocomposite with wavelength.

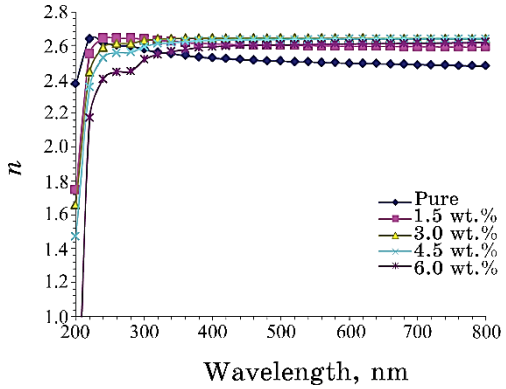

Fig. 7. Variation of refractive index of PEO/PVA/Fe_2O_3 nanocomposites with wavelength.

weight percentages of Fe_2O_3 nanoparticles [34, 35]. The extinction coefficient has high values at UV region; this behaviour is attributed to high absorbance of all samples of nanocomposites [36]. Also, extinction coefficient of nanocomposites increases with the increasing of the wavelength at visible and near-infrared regions that is attributed to the absorption coefficient of nanocomposites, which is approximately constant at visible and near-infrared region; hence, the extinction coefficient increases with increasing of the wavelength [36–38].

The refractive index of PEO/PVA/Fe_2O_3 nanocomposites as a function of wavelength is shown in Fig. 7. It can be seen that the refractive index increases with increasing the weight percentages of the concentration of Fe_2O_3 nanoparticles. In addition, it is decreased with the increase of the wavelength. This behaviour is attributed to the increase of the density of nanocomposites. When the incident light interacts with a sample, refractivity at UV region is high; hence, the values of refractive index will be increased [39, 40].

3.4. Real and Imaginary Parts of Dielectric Constant

Figure 8 shows the change of ε_1 as a function of the wavelength for PEO/PVA/Fe_2O_3 nanocomposites. It can be seen that ε_1 depends considerably on n^2 due to low value of k^2; so, the real dielectric constant is increased with the increase of the concentration of Fe_2O_3 nanoparticles.

Figure 9 shows the change of ε_2 as a function of the wavelength. It can be seen that ε_2 is dependent on k values, which is changed with changing the absorption coefficient due to the relation between

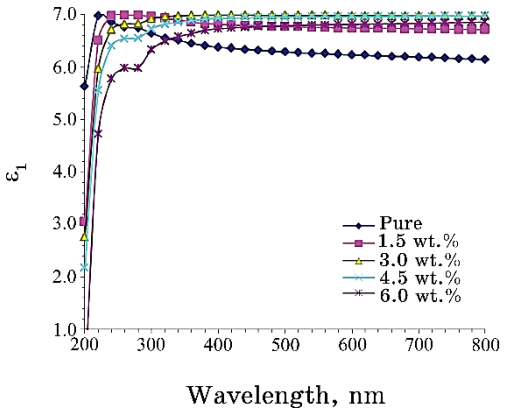

Fig. 8. Variation of real part of dielectric constant for the PEO/PVA/Fe_2O_3 nanocomposites with wavelength.

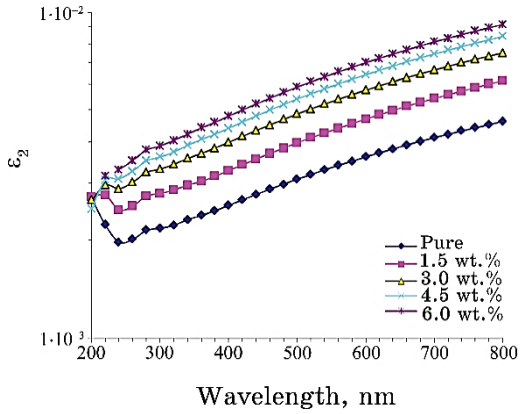

Fig. 9. Variation of imaginary part of dielectric constant for the PEO/PVA/Fe_2O_3 nanocomposites with wavelength.

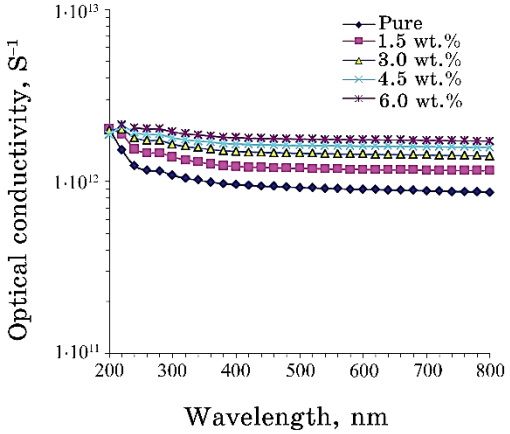

Fig. 10. Variation of optical conductivity for the PEO–PVA–Fe_2O_3 nanocomposites with wavelength.

α and k. This behaviour is consistent with the results of Refs. [41, 42].

3.5. Optical Conductivity of PEO/PVA/Fe_2O_3 Nanocomposites

Figure 10 shows that the relationship between optical conductivity of PEO/PVA/Fe_2O_3 nanocomposites and wavelength. The optical conductivity for all samples of nanocomposites is decreased with the increasing the wavelength; this behaviour is attributed to the optical-conductivity dependence on the wavelength of the radiation incident on the samples of nanocomposites; the increase of optical

conductivity at a low wavelength of photon is due to high absorbance of all samples of nanocomposites in this region and, hence, increase of the charge-transfer excitations [43]. In addition, the optical conductivity of nanocomposites is increased with the increase of Fe_2O_3 nanoparticles' concentration that is related to the increase of the absorption coefficient and, consequently, increasing the optical conductivity of PEO/PVA/Fe_2O_3 nanocomposites [44].

3.6. Application of PEO/PVA/FE_2O_3 Nanocomposites for Antibacterial Activity

Figure 11 shows the variation of inhibition zone diameter with Fe_2O_3 nanoparticles' concentration against *Escherichia coli* for the PEO/PVA/Fe_2O_3 nanocomposites. In this figure, the inhibition zone increases with increasing concentration of Fe_2O_3 nanoparticles. The reason for the antibacterial activity of PEO/PVA/Fe_2O_3 nanocomposites may be due to the presence of reactive oxygen species (ROS) produced with different concentrations of Fe_2O_3 nanoparticles.

The reason for the nanocomposites' antibacterial activity could be the chemical interaction between hydrogen peroxide and membrane [45, 46].

The produced hydrogen peroxide enters and kills the cell membrane of bacteria. The other possible mechanism of action is that the Fe_2O_3 nanoparticles in nanocomposites carry the positive charges, and the microbes have the negative charges, which create the electromagnetic attraction between the nanoparticles and the microbes. When the attraction is created, the microbes become oxidized, and they die instantly [47].

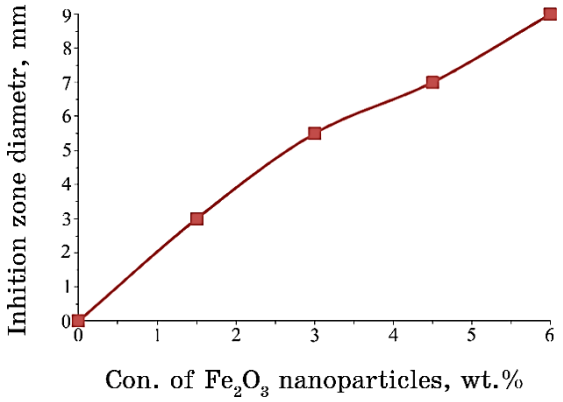

Fig. 11. Variation of inhibition zone diameter with Fe_2O_3 nanoparticles' concentration against *Escherichia coli* for the PEO/PVA/Fe_2O_3 NCs.

4. CONCLUSIONS

PEO/PVA as the host polymer-blend matrix was doped with iron-oxide nanoparticles using a casting technique to make new and low-end optoelectronic nanocomposites. By increasing iron-oxide nanoparticles' concentration, PEO/PVA/Fe_2O_3 nanocomposites absorb more light. The absorbance of PEO/PVA/Fe_2O_3 NCs increases with increasing of concentration of Fe_2O_3 nanoparticles, while transmittance decreases. The energy gap of PEO/PVA blend was drop from 3.79 eV to 3.38 eV and from 2.79 eV to 2.18 eV for allowed and forbidden indirect transitions, respectively, when the ratio of iron-oxide nanoparticles reached 6 wt.%. With increasing concentration of Fe_2O_3 nanoparticles, the extinction coefficient, absorption coefficient, refractive index, imaginary and real parts of dielectric constant and optical conductivity are increasing. With increasing frequency, the dielectric loss and dielectric constant drop, while the alternating-current electrical conductivity rises. The experimental results on antibacterial activity show that the inhibition zone diameter of nanocomposites increases with increasing of Fe_2O_3 nanoparticles' concentration. These results confirm the potential employee of these materials in optoelectronics fields such as light filters, transistors, sensors, diodes, lasers, electronics gates and in food packaging industries.

REFERENCES

1. S. L. Jangra, K. Stalin, N. Dilbaghi, S. Kumar, J. Tawale, Surinder P. Singh, and Renu Pasricha, *Journal of Nanoscience and Nanotechnology*, **12**: 7105 (2012).
2. D. R. Paul and L. M. Robeso, *Polymer*, **49**, No. 15: 3187 (2008).
3. H. N. Obaid, M. A. Habeeb, F. L. Rashid, and A. Hashim, *Journal of Engineering and Applied Sciences*, **8**, No. 5: 143 (2013); doi:10.36478/jeasci.2013.143.145
4. B. S. Mudigoudra, S. P. Masti, and R. B. Chougale, *Research Journal of Recent Sciences*, **1**, No. 9: 83 (2012); https://www.researchgate.net/publication/284506738_Thermal_Behavior_of_Poly_vinyl_alcoholPoly_vinyl_pyrrolidone_Chitosan_Ternary_Polymer_Blend_Films
5. M. A. Habeeb, *European Journal of Scientific Research*, **57**, No. 3: 478 (2011).
6. Sagadevan Suresh, *American Chemical Science Journal*, **3**, No. 3: 325 (2013); doi:10.9734/ACSJ/2013/3503
7. M. A. Habeeb and Z. S. Jaber, *East European Journal of Physics*, **4**: 176 (2022); doi:10.26565/2312-4334-2022-4-18
8. T. S. Soliman and S. A. Vshivkov, *J. Non-Cryst. Solids*, **519**: 119452 (2019); https://doi.org/10.1016/j.jnoncrysol.2019.05.028
9. A. H. Hadi and Majeed Ali Habeeb, *Journal of Mechanical Engineering Re-*

search an Developments, **44**, No. 3: 265 (2021); https://jmerd.net/03-2021-265-274
10. N. Manavizadeh, A. Khodayari, and E. Asl-Soleimani, *Proceedings of ISES World Congress*, **1**: 1120 (2008); https://doi.org/10.1007/978-3-540-75997-3_220
11. Q. M. Jebur, A. Hashim, and M. A. Habeeb, *Egyptian Journal of Chemistry*, **63**: 719 (2020); https://dx.doi.org/10.21608/ejchem.2019.14847.1900
12. T. Siddaiah, P. Ojha, N. O. Kumar, and C. Ramu, *Mater. Res.*, **21**, No. 5: 321 (2018); https://doi.org/10.1590/1980-5373-mr-2017-0987
13. S. M. Mahdi and M. A. Habeeb, *Optical and Quantum Electronics*, **54**, No. 12: 854 (2022); https://doi.org/10.1007/s11082-022-04267-6
14. C. Uma Devi, A. K. Sharma, and V. V. R. N. Rao, *Materials Letters*, **56**, No. 3: 167 (2002); https://doi.org/10.1016/S0167-577X(02)00434-2
15. N. Hayder, M. A. Habeeb, and A. Hashim, *Egyptian Journal of Chemistry*, **63**: 577 (2020); doi:10.21608/ejchem.2019.14646.1887
16. V. Ghorbani, M. Ghanipour, and D. Dorranian, *Opt. Quant. Electron*, **48**: 61 (2016); https://doi.org/10.1007/s11082-015-0335-7
17. M. A. Habeeb, A. Hashim, and N. Hayder, *Egyptian Journal of Chemistry*, **63**: 709 (2020); https://dx.doi.org/10.21608/ejchem.2019.13333.1832
18. S. Kramadhati and K. Thyagarajan, *Int. Journal of Engineering Research and Development*, **6**, No. 8: 167 (2013).
19. A. Hashim, M. A. Habeeb, and Q. M. Jebur, *Egyptian Journal of Chemistry*, **63**: 735 (2020); https://dx.doi.org/10.21608/ejchem.2019.14849.1901
20. S. Choudhary, *J. Phys. Chem. Solids.*, **121**: 196 (2018); https://doi.org/10.1016/j.jpcs.2018.05.017
21. A. H. Mohammed and M. A. Habeeb, *HIV Nursing*, **22**, No. 2: 1167 (2022); https://doi.org/10.31838/hiv22.02.225
22 Mohammad Rezvanpour, Mahdi Hasanzadeh, Danial Azizi, Alireza Rezvanpour, and Mohammad Alizadeh, *Mater. Chem. Phys.*, **215**: 299 (2018); https://doi.org/10.1016/j.matchemphys.2018.05.044
23. S. M. Mahdi and M. A. Habeeb, *Physics and Chemistry of Solid State*, **23**, No. 4: 785 (2022); doi:10.15330/pcss.23.4.785-792
24. M. Chirita and I. Grozescu, *Chem. Bull. 'POLITEHNICA' Univ. (Timişoara)*, **54**, No. 68: 1 (2009); https://www.researchgate.net/profile/Chirita-Marius/publication/228924462_1_Fe_2_O_3-Nanoparticles_Physical_Properties_and_Their_Photochemical_And_Photoelectrochemical_Applications/links/55801afa08ae47ede114da7e/1-Fe-2-O-3-Nanoparticles-Physical-Properties-and-Their-Photochemical-And-Photoelectrochemical-Applications.pdf
25. M. A. Habeeb and W. S. Mahdi, *International Journal of Emerging Trends in Engineering Research*, **7**, No. 9: 247 (2019); doi:10.30534/ijeter/2019/06792019
26 T. S. Soliman and S. A. Vshivkov, *J. Non-Cryst. Solids*, **519**: 119452 (2019); https://doi.org/10.1016/j.jnoncrysol.2019.05.028
27. Z. I. Zike and M. A. Habeeb, *HIV Nursing*, **22**, No. 2: 1185 (2022); https://doi.org/10.31838/hiv22.02.229
28. M. Ghanipour and D. Dorranian, *Journal of Nanomaterials*, **2013**: Article ID 897043 (2013); https://doi.org/10.1155/2013/897043

29. M. A. Habeeb and R. S. Abdul Hamza, *Journal of Bionanoscience*, **12**, No. 3: 328 (2018); https://doi.org/10.1166/jbns.2018.1535
30. S. Ramesh and L. C. Wen, *Ionics (Kiel)*, **16**, No. 3: 255 (2010); https://doi.org/10.1007/s11581-009-0388-3
31. M. A. Habeeb, A. Hashim, and N. Hayder, *Egyptian Journal of Chemistry*, **63**: 697 (2020); https://dx.doi.org/10.21608/ejchem.2019.12439.1774
32. S. Kramadhati and K. Thyagarajan, *Int. Journal of Engineering Research and Development*, **6**, No. 8: 15 (2013); https://www.ijerd.com/paper/vol6-issue8/D06081921.pdf
33. N. K. Abbas, M. A. Habeeb, and A. J. K. Algidsawi, *International Journal of Polymer Science*, **2015**: 926789 (2015); https://doi.org/10.1155/2015/926789
34. A. Goswami, A. K. Bajpai, and B. K. Sinha, *Polym. Bull.*, **75**, No. 2: 781 (2018); https://doi.org/10.1007/s00289-017-2067-2
35. M. A. Habeeb and W. K. Kadhim, *Journal of Engineering and Applied Sciences*, **9**, No. 4: 109 (2014); doi:10.36478/jeasci.2014.109.113
36. A. Choudhary, *J. Phys. Chem. Solids*, **2018**, No. 121: 196 (2018); https://doi.org/10.1016/j.jpcs.2018.05.017
37. M. A. Habeeb, *Journal of Engineering and Applied Sciences*, **9**, No. 4: 102 (2014); doi:10.36478/jeasci.2014.102.108
38. Goutam Chakraborty, Kajal Gupta, Dipak Rana, and Ajit Kumar Meikap, *Advances in Natural Sciences: Nanoscience and Nanotechnology*, **4**, No. 2: 025005 (2013); doi:10.1088/2043-6262/4/2/025005
39. A. H. Hadi and M. A. Habeeb, *Journal of Physics: Conference Series*, **1973**, No. 1: 012063 (2021); doi:10.1088/1742-6596/1973/1/012063
40. R. Tintu, K. Saurav, K. Sulakshna, V. P. N. Nampoori, P. Radhakrishnan, and S. Thomas, *J. Non-Oxide Glas.*, **2**, No. 4: 167 (2010).
41. S. M. Mahdi and M. A. Habeeb, *Digest Journal of Nanomaterials and Biostructures*, **17**, No. 3: 941 (2022); https://doi.org/10.15251/DJNB.2022.173.941
42. C. Uma Devi, A. K. Sharma, and V. V. R. N. Rao, *Materials Letters*, **56**, Iss. 3: 167 (2002); https://doi.org/10.1016/S0167-577X(02)00434-2
43. Q. M. Jebur, A. Hashim, and M. A. Habeeb, *Egyptian Journal of Chemistry*, **63**, No. 2: 611 (2020); https://dx.doi.org/10.21608/ejchem.2019.10197.1669
44. Y. T. Prabhu, K. V. Rao, B. Siva Kumari, V. S. S. Kumar, T. Pavani, *International Nano Letters*, **5**, No. 2: 85 (2015); doi:10.1007/s40089-015-0141-z
45. M. A. Habeeb and R. S. A. Hamza, *Indonesian Journal of Electrical Engineering and Informatics*, **6**, No. 4: 428 (2018); doi:10.11591/ijeei.v6i1.511
46. L. Kungumadevi, R. Sathyamoorthy, and A. Subbarayan, *Solid. State. Electron.*, **54**, 1: 58 (2010); doi:10.1016/j.sse.2009.09.023
47. S. R. Kumar, R. G. Krishnan, *International Journal of Pharmaceutical Sciences and Drug Research*, **4**, No. 2: 157 (2012); http://ijpsdr.com/index.php/ijpsdr/article/view/209